IEEE Access
Multidisciplinary | Rapid Review | Open Access Journal

Received April 6, 2021, accepted April 23, 2021, date of publication April 27, 2021, date of current version May 4, 2021.

Digital Object Identifier 10.1109/ACCESS.2021.3076000

A Method for Rapid Measurement of the Deformation and Spatial Attitude of Large Radar Antennas Inside Radomes

XIAO GUAN, YAMING XU, AND CHENG XING
School of Geodesy and Geomatics, Wuhan University, Wuhan 430079, China

Corresponding author: Cheng Xing (chxing@sgg.whu.edu.cn)

This work was supported in part by the Changjiang River Scientific Research Institute Open Research Program under Grant CKWV2017518/KY, and in part by the Natural Science Foundation of Hubei Province under Grant 2017CFB654.

ABSTRACT It is challenging to measure, analyze, and control the deformation and space attitude of antennas in narrow radomes through geometric measurement to ensure the accuracy of phased array radar application. In this manuscript, a method for rapid measurement of antennas by adopting the combination of photogrammetry system, laser tracker and total station was proposed. The photogrammetric method was used with a homemade auxiliary tool to measure and calculate the antenna's deformation under different temperatures and pitch angles. Mapping relations between the instrumental coordinate systems of photogrammetry system, laser tracker and total station were established through common points, including target balls and reflectors. Coordinates of mark points on antenna surface were converted from photogrammetric coordinate system to laser tracker's and total station's coordinate system. Thus, antenna's pitch angles relative to the local horizontal plane and deflection angles relative to the north of the engineering coordinate system were calculated. Planar fitting, coordinate transformation and space attitude calculation were all carried out in the Spatial Analyzer (SA) software. The photogrammetric method detected the antenna's gravitational deformation sensitively, the maximum Root Mean Square Residual (RMSR) of the reference length was 54 μm, and that of the mark points was 59 μm, which was stably in line with its nominal accuracy. Deviations caused by coordinate transformation had no significant effect on the calculation of antenna's spatial attitude, for the maximum deviation between the converted and measured coordinates in laser tracker's coordinate system was 0.139 mm, and that in total station's coordinate system was 1.037 mm, both of which were within reasonable limits of the derived theoretical maximum deviations between different instruments. As a result, the maximum deviation between the calculated value and servo system's nominal value of antenna's pitch angle was 59.4″, and that of antenna's deflection angle was 91.87″. This method's efficiency was greatly improved by about ten times compared with traditional methods through statistics and estimates.

INDEX TERMS Coordinate transformation, flatness, laser tracker, photogrammetry system, spatial attitude, total station.

I. INTRODUCTION

Phased array radar is a phase-controlled electronically scanning radar whose antenna array consists of many radiation units and receiving units. These units are arranged regularly on a plane to form an array of the antenna [1]–[4].

Operational radars are usually equipped with a radome to reduce the antenna's environmental effects and allow continuous operation under bad weather conditions [5]. However, the main beam's homogeneity with respect to differential power and phase is degraded with the radome [6]. The radio frequency performance of a radome is affected by different conditions, including dirtiness, wetness, and varying temperature [7]. For instance, rainfall or a continuous water layer on a radome may lead to transmission loss, attenuation, reflections, or cross polarization [8]–[10]. However, radome-induced azimuthal variability of the radar could be negligible [6]. Meteorological requirements met by radars may impact the design of antenna, transmitter-receiver, and signal processor [11].

The associate editor coordinating the review of this manuscript and approving it for publication was Wuliang Yin.

Besides the environmental effects on the radome, a large antenna structure inevitably is affected by gravity, temperature and other factors. The resulting structure deformation changes the planar degree and polarization direction of the array surface, resulting in beam distortion, pointing deflection, gain decrease, and side lobe rise [12]–[14]. Therefore, the analysis and compensation of the influence of structural deformation on electrical performance have been a research hotspot for a long time [15]–[17]. According to the theoretical knowledge, antenna performance is related to the root mean square value of its structural error, but not determined by the maximum error of individual points. Nowadays, as the working frequency band and the aperture of the antenna increase, the requirements on the precision of the form surface has become more and more stringent, and the simple design of the conformal structure has been unable to meet the requirements of high precision [18]–[20]. On the other hand, the antenna's servo system directly controls its spatial attitude, including the pitch angle relative to the local horizontal plane and the deflection angle relative to the engineering coordinate system's north direction. The error of the servo system directly causes the pointing deviation of the antenna [21]. Therefore, it is significant to correctly analyze and control the antenna's deformation and spatial attitude in phased array radar application.

Form surface measurement technology of large-aperture antenna has always been one of the research hotspots [22]. For example, the form surface of Lovell 76m of the UK [23] was initially measured by the method of transit-steel tape or the improved ones [24]. The total station was used in the form surface measurement of Japan's Nobeyama45m [25]. The form surface measurement and adjustment of America's GBT100m [26], Arecibo305m [27] and China's FAST500m [28] adopted more advanced technologies such as laser measurement, photogrammetry and microwave holography.

There are few types of research on the technology of attitude measurement for the large-aperture antennas. In typical engineering projects, total stations or double theodolite systems are always adopted to directly measure the three-dimensional coordinates of points on the antenna, with a certain number of observation marks pasted on the antenna surface. Then the antenna could be fitted, and its attitude parameters in space are obtained.

In this manuscript, the phased array radar antenna has an aperture of 13 meters and a radome outside it. The space inside the radome is narrow, as the distance between the base track of the antenna and the wall is only about 2 meters. The following measurement work would be completed:

(1) Detection of the antenna deformation under different temperature and pitch angles, which is judged by the antenna's flatness. The temperature conditions were set in four groups as 5°C, 8°C, 12°C, and 25°C. The pitch angles of the servo system were set in six groups as 0°, 15°, 30°, 45°, 60°, and 75°. It was defined that the pitch angle of the antenna in the vertical state was 0°.

(2) Calculation of the antenna's spatial attitude, including the pitch angles relative to the local horizontal plane and the deflection angles relative to the north direction of the engineering coordinate system, and the deviation between the set angles of the servo system and the calculated angles. The engineering coordinate system in this manuscript is composed of Gauss-Krueger plane rectangular coordinate system and an independent elevation system.

In allusion to the scenes and requirements of the measurement in this manuscript, the traditional methods might have the following disadvantages:

(1) The space for instrument erection in the radome is very limited. Obstacles are everywhere, leading to poor visibility of measurement points.

(2) The photogrammetric results belong to an independent photogrammetric coordinate system and cannot be included in the engineering coordinate system.

(3) The photogrammetric results lack external validation values, so only the precision of inner coincidence can be obtained, but its precision of external coincidence cannot be known.

(4) Due to the limitations such as depth of field of the industrial measuring camera, reflection angle of photographic marks, size of the antenna, and pitch angle, a blind area is likely to appear during measurement.

(5) The ratio of antenna size to the length of the photogrammetric reference ruler is too large, which is not conducive to global control of the scale precision.

(6) There is the function ''Unified Spatial Metrology Network'' (USMN) in the SA software, which can combine a variety of measuring instruments for combined measurement, such as photogrammetry, laser tracker, total station. However, the instrument models supported by the software are limited. In this manuscript, the models of photogrammetry system and total station we carried were not supported, so this function could not be directly used.

(7) If only a total station were used for observation, not only would the efficiency be reduced due to the excessive number of observation marks, but also when the antenna is at a high pitch angle, the total station could not directly observe the points on the antenna surface due to the narrow space in the radome.

In this work, our major contributions are as follows:

(1) The combination of photogrammetry system, laser tracker and total station was adopted, not only solving the targeting problem of laser tracker and total station when the antenna was at a high pitch angle, but also greatly improving the measurement efficiency by about ten times comparing with the traditional methods.

(2) As there was no available manned equipment, an extension bar tooling was made to help extending the camera's measuring range and taking images of the full range of the antenna plane, solving the problem of camera sampling when the antenna was at a high pitch angle. Results showed that the tool had good stability.

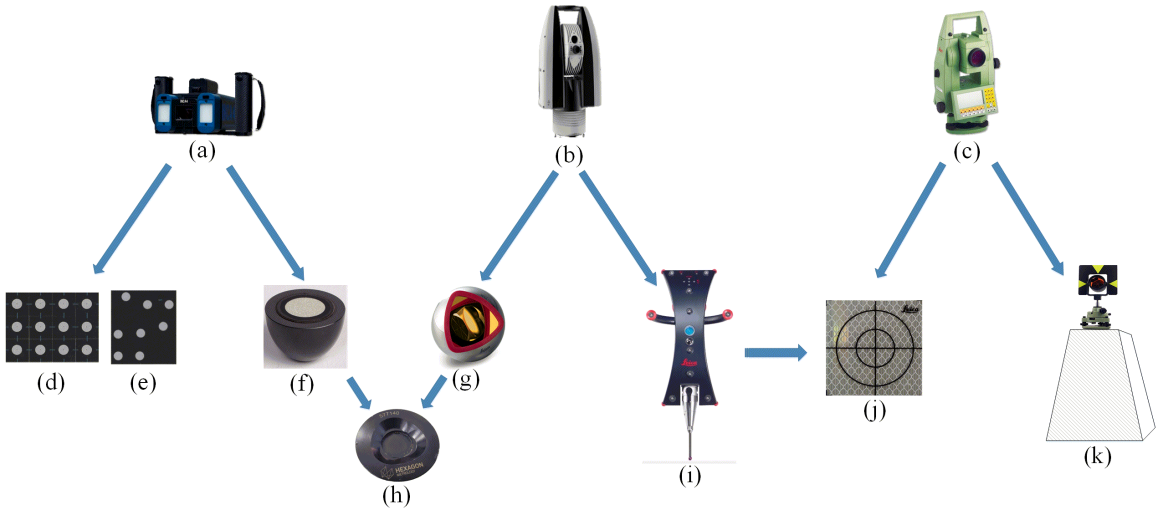

FIGURE 1. Observation instruments and marks: (a) photogrammetry system; (b) laser tracker; (c) total station; (d) photogrammetric mark points; (e) photogrammetric code points; (f) photogrammetric target ball; (g) laser tracker's target ball; (h) magnetic base; (i) Leica's handheld wireless T-probe; (j) reflector; (k) prism. The arrows indicate the correspondence between observation instruments and marks. Centre of the photogrammetric target ball (f) and laser tracker's target ball (g) were unified by magnetic base (h).

(3) Mapping relations between instruments' coordinate systems were established by target balls, reflectors, and Leica's handheld probe, and coordinate transformations were done by the best-fit function in SA software as the Unified Spatial Metrology Network (USMN) could not be adopted.

(4) The theoretical maximum deviations of observations between different instruments were derived, giving a reasonable explanation for the deviations caused by coordinate transformation.

II. MATERIALS AND METHODS

A. OBSERVATION INSTRUMENTS AND MARKS

In this survey, the photogrammetry system V-Stars/INCA4 from GSI was adopted for the photogrammetric measurement with the nominal accuracy of 4 μm + 4 μm /m. The laser tracker was LEICA AT960 with a nominal accuracy of 15 μm + 6 μm/m, equipped with Leica's handheld wireless T-Probe, which has a nominal accuracy of no more than 60 μm within a measuring range of 8.5 meters. The total station was LEICA TS60 with the nominal ranging accuracy of 0.6 mm + 1 ppm and angular measurement accuracy of 0.5″.

Five kinds of observation marks were adopted, including photogrammetric marks, photogrammetric target balls, laser tracker target balls, reflectors, and prisms. The two kinds of target balls were of the same size and served as common points of the photogrammetry system and laser tracker by unifying the balls' centre by fixed magnetic bases. The reflectors served as the common points of total station and laser tracker. The common points helped to establish mapping relations between coordinate systems of the three instruments.

There were four observation piers outside the radome on which forced centring marks were set, whose names are Pe, Pw, Ps, and Pn, with their coordinates in the engineering coordinate system already known. There was also a forced centring observation pier inside the radome, on which the observation mark is named Pi, with unknown coordinates. Beside Pi, there was a window on the radome wall, through which the pier Ps could be seen. The distribution of the four observation piers is shown in Fig. 2.

B. LAYOUT OF OBSERVATION MARKS, INSTRUMENTS AND AUXILIARY TOOLS

Due to the limited space and the complex distribution of mechanical equipment within the radome, it was necessary to select positions with good visibility conditions and appropriate observation angle for the instruments. In addition, to improve the precision of coordinate transformation, the common observation points should be uniformly distributed in three-dimensional space. According to the above principles and actual site conditions, five reflectors were fixed on the inner wall and ground inside the radome, whose names are K1, K2, K3, K4, and K5. Five magnetic ball bases named S1, S2, S3, S4, and S5 were fixed on the side of the antenna base, as shown in Fig. 2.

The antenna plane is formed by units arranged regularly on a plane. In this work, since the unit is square, we defined midpoint of each side of the unit as the key points, on which photogrammetric marks were pasted. Photogrammetric marks were uniformly laid out on the antenna surface from top to bottom and from left to right, so as to ensure that there are at least 12 mark points and 4 encoded points on each photo [29]. To ensure that the position of the five target balls on the antenna base can be correlated with the photogrammetric marks in the state of a high pitch angle, so as to complete the photo splicing in photogrammetric calculation, a certain

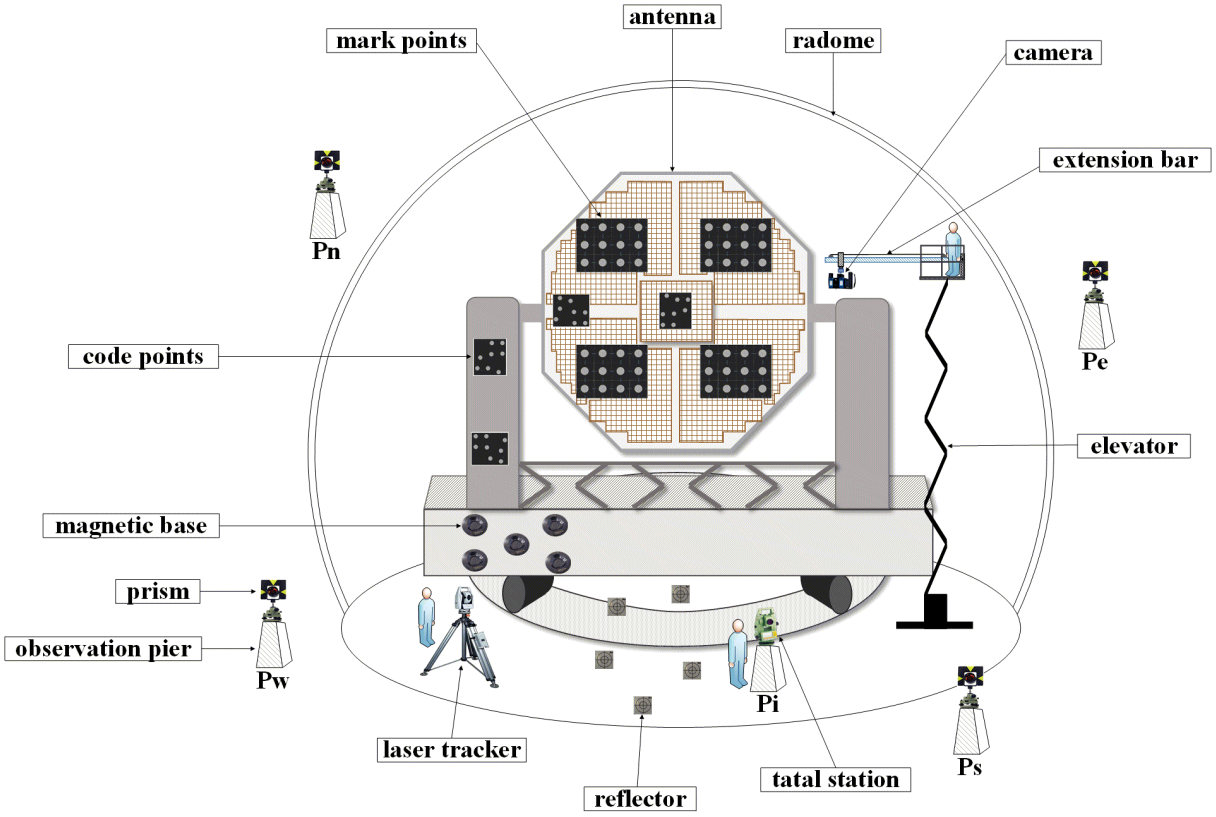

FIGURE 2. Layout of observation marks (photogrammetric mark points and code points, magnetic bases on which the target balls were attached, reflectors, and prisms on observation piers), instruments (camera, laser tracker, and total station), and auxiliary tools (elevator and extension bar) in and out of the radome.

number of encoded points were also laid on the bottom and back of the antenna. A total of 795 photogrammetric mark points were laid out on the antenna surface, named B1-B795.

The antenna is large, but the radome's elevator could only move vertically and horizontally for its base is fixed. So, if the antenna is at a high pitch angle and the elevator rises to a high altitude, the surveyor on the elevator is close to the lower part of the antenna but too far from the upper part, so that he is not able to take images of all the mark points on the antenna surface, and the photogrammetric shooting angle is too big at the same time. In order to overcome this problem, an extension bar tooling was made to assist the photogrammetric measurement. The extension bar is composed of three 2-meter-long aluminum bar pieces connected by connectors, with a total length of six meters and a sliding device installed above. In the process of measurement, the extension bar was fixed on the elevator while the camera was fixed on the sliding device. We pulled the sliding device by the steel wire rope so that the camera could reach any position on the extension bar. With the help of the remote shutter of the camera, the full range of the antenna plane could be measured.

C. OBSERVATION METHOD

In this measurement, the antenna's deflection angle was set constantly at 150° by the servo system. And we successively set the temperatures at 5°C, 8°C, 12°C, 25°C and the antenna's pitch angles at 0°, 15°, 30°, 45°, 60°, 75°. At a certain temperature, the antenna was flipped from 0° to 75° successively, and the measurement was done at each pitch angle. After completing six sets of measurements, the temperature condition was reset to another, and the antenna was rotated horizontally once and returned to the deflection angle of 150°. Thus, a total of $4*6 = 24$ groups of observations were obtained. Each group had 5 total station's observations (coordinates of 5 reflectors), 10 laser tracker's observations (coordinates of 5 reflectors and 5 laser tracker's target balls) and 800 photogrammetric observations (coordinates of 5 photogrammetric target balls and 795 photogrammetric mark points).

1) MEASUREMENT BY PHOTOGRAMMETRY SYSTEM

Five 1.5 inch (38.1 mm) photogrammetric target balls were fixed to the five magnetic bases, with the direction of the reflective marks at the centre adjusted to face towards the camera. Under different conditions of temperature and pitch angles, we took photos of the antenna surface about 8 to 10 meters away from the antenna, holding the INCA4 industrial camera and adjusting the measuring position by the elevator. Images including 795 photogrammetric marks B1-B795 and 5 target balls S1-S5 were obtained.

There were two one-meter-long reference rulers in the V-Stars' accessories. However, as the antenna is with a

diameter of 13 meters, the distance between the target balls measured by laser tracker was used instead as the reference in the photogrammetric calculation, which could help obtain a better length constraint.

After the image files were imported to the computer, the supporting software of V-Stars was used for image processing and calculation. The bundle adjustment was adopted to calculate the camera's internal and external orientation elements and the coordinates of the mark points. Then the three-dimensional coordinates of 795 mark points and 5 target balls in the photogrammetric coordinate system were obtained.

2) MEASUREMENT BY LASER TRACKER

To measure and calculate the pitch angle of the antenna relative to the local horizontal plane, we roughly levelled the laser tracker. We then set up a horizontal plane measured by the built-in gradienter of the laser tracker whose nominal accuracy is $\pm 1''$ and the function ''Gravity Reference Measurement'' of the SA software. Thus, a spatial rectangular coordinate system was established in which this horizontal plane was the XOY plane and set as the laser tracker's working coordinate system. Then the laser tracker's target ball was successively placed on the five magnetic bases and measured. Leica's wireless handheld T-Probe mounted with a 0.1 mm probe was adopted to measure the reflectors, by placing the probe's tip stably on the cross-section centre of the reflector, as shown in Fig. 3.

FIGURE 3. The way in which the laser tracker aimed at the reflector via the handheld T-probe.

The antenna base was fixed, so the target balls' positions were constant when the pitch angle of the antenna changed. Therefore, under each temperature condition, while the antenna flipped from 0° to 75°, the laser tracker measured the coordinates of S1-S5 only once. Then the three-dimensional coordinates of 5 target balls and 5 reflectors under the laser tracker's coordinate system were obtained.

3) MEASUREMENT BY TOTAL STATION

Firstly, we set up the total station on the pier Ps and prisms on Pi and Pe. As the coordinates of Pe and Ps were already known, after taking the height of the total station and prisms, we took the prism on Pe as the orientation point and measured the prism on Pi, thus obtained the coordinates of Pi in the total station's coordinate system.

Secondly, we set up the total station on the pier Pi and measured the height of it. As the coordinates of Pi had been obtained in the first step, we took the prism on Ps as the orientation point and measured the 5 reflectors K1-K5, thus obtained their coordinates in the total station's coordinate system.

The reflectors were fixed on the wall and the ground, so they were not affected by the antenna's attitude change. Thus, their coordinates were measured only once by the total station for all the 24 group observations.

D. CALCULATION METHOD

1) CALCULATION OF ANTENNA'S FLATNESS

An ideal plane was fitted with the minimum sum of the square of the distance from the observation points, so as to calculate the flatness value of the measured plane [30]. Coordinates of the 795 photogrammetric mark points calculated by the V-Stars software were imported to the SA software and used to fit the antenna plane. Thus, the antenna's flatness parameter was obtained.

2) COORDINATE TRANSFORMATION

The SA software successively converted coordinates of mark points on the antenna surface from the photogrammetric coordinate system to the laser tracker and total station's coordinate systems. Taking one group of observations as an example, the method is as follows.

Firstly, photogrammetric observations (including 795 mark points B1-B795 and 5 target balls S1-S5) and laser tracker's observations of 5 target ball S1-S5 were imported to the SA software. A best-fit transformation was done, taking the laser tracker's observations S1-S5 as the reference, while photogrammetric observations S1-S5 were the corresponding values. Thus, coordinates of photogrammetric observations B1-B795 were converted to the laser tracker's coordinate system.

Secondly, the laser tracker's observations (including 795 converted mark points B1-B795 and 5 reflectors K1-K5) and total station's observations of 5 reflectors K1-K5 were imported to the SA software. A best-fit transformation was performed, taking the total station's observations K1-K5 as the reference, while the laser tracker's observations K1-K5 were the corresponding values. Thus, coordinates of laser tracker's observations B1-B795 were converted to the total station's coordinate system, namely the engineering coordinate system. Then the antenna's attitude under the engineering coordinate system could be calculated.

3) CALCULATION OF ANTENNA'S PITCH ANGLES AND DEFLECTION ANGLES

Calculation of the antenna's attitude was also done in the SA software. On the one hand, we fitted the antenna plane by the 795 mark points B1-B795 in the laser tracker's coordinate system, and obtained the normal of the plane. As mentioned above, the XOY plane of the laser tracker's coordinate system represented the local horizontal plane. Then we queried the angle between the normal line and XOY plane, which is the angle between the antenna's normal direction and the local horizontal plane, namely the antenna's pitch angle.

On the other hand, we fitted the antenna plane by the 795 mark points B1-B795 in the total station's coordinate system, obtained the normal of the plane, and projected the normal line onto the XOY plane. As the positive X-axis represented the north direction of the engineering coordinate system, we queried the angle between the normal line's projection and the positive X-axis, which is the angle between the antenna's normal direction and the north direction of the engineering coordinate system, namely the antenna's deflection angle.

III. RESULTS

A. ANTENNA'S FLATNESS

The flatness parameters of the antenna were expressed by RMS or flatness. The RMS represents the root mean square value of the distance between the points and the fitting plane, while the flatness represents the maximum deviation of the macroscopic concave-convex height of the actual plane relative to the ideal plane. The flatness parameters of the 24 groups of fitting planes are shown in Table 1.

TABLE 1. Calculation results of antenna's flatness.

Temperature	Pitch angle	RMS (mm)	Flatness (mm)
5°C	0°	0.563	4.803
	15°	0.672	5.487
	30°	0.821	6.287
	45°	0.999	7.045
	60°	1.15	7.531
	75°	1.261	7.596
8°C	0°	0.575	4.808
	15°	0.679	5.546
	30°	0.838	6.291
	45°	1.004	7.023
	60°	1.155	7.400
	75°	1.280	7.386
12°C	0°	0.591	4.710
	15°	0.709	5.496
	30°	0.830	6.102
	45°	1.009	6.972
	60°	1.138	7.281
	75°	1.234	7.374
25°C	0°	0.554	4.186
	15°	0.624	4.629
	30°	0.755	5.410
	45°	0.907	5.943
	60°	1.058	6.518
	75°	1.126	6.477

It can be seen from Table 1 that the antenna's flatness presents a certain regular change. On the one hand, at the same temperature, the larger the antenna's pitch angle is, the greater the value of its flatness is. On the other hand, change of temperature did not significantly affect the antenna's flatness. This can be explained that the flatness is determined by the relative positions of the units that make up the antenna plane. Due to gravity's effect, different degree of settlement occurs in units of different parts. Thus, the larger the antenna's pitch angle is the greater the antenna's deformation. But temperature would not have a significant effect on this. It is consistent with our normal cognition. The results indicate that the photogrammetry system was able to detect the deformation of the antenna sensitively under such measuring conditions.

B. ANTENNA'S ATTITUDE

Deviations between the calculated attitude and the servo system's nominal values under different temperatures and pitch angles were also calculated, as shown in Table 2.

TABLE 2. Deviations between antenna's calculated attitude and servo system's nominal values.

Temperature	Servo system's nominal deflection angles	Deviations of calculated deflection angles(″)	Servo system's nominal pitch angles	Deviations of calculated pitch angles(″)
5°C	150°	57.52	0°	40.32
		46.96	15°	45.48
		32.29	30°	50.76
		18.45	45°	39.00
		-14.81	60°	10.08
		-56.61	75°	27.72
8°C	150°	9.63	0°	46.32
		-10.05	15°	8.64
		-21.51	30°	24.12
		-36.64	45°	59.40
		-66.04	60°	-11.88
		-91.87	75°	11.88
12°C	150°	42.83	0°	6.96
		10.59	15°	47.28
		-7.93	30°	31.68
		-14.94	45°	18.84
		-42.43	60°	2.52
		-61.03	75°	30.96
25°C	150°	23.59	0°	54.60
		11.54	15°	41.40
		4.01	30°	49.32
		-9.74	45°	29.16
		-18.22	60°	44.28
		-23.59	75°	24.48

On the one hand, the maximum deviation of pitch angles was 59.4″. Deviations of pitch angles did not show apparent regularity with the change of the antenna's pitch angle.

On the other hand, the maximum deviation of deflection angles was 91.87″. With the increase of the antenna's pitch angle, the deviations between the calculated deflection angles and the servo system's nominal values showed a systematic change from positive to negative, and the absolute value decreased first and then increased. The minimum absolute value was 0.4″.

Therefore, it could be inferred that the deviations of the pitch angles show irregular changes because they are mainly caused by the random error of measurement. While the deviations of the deflection angles reflect that the horizontal rotation axis around which the antenna was pitching is not parallel to the XOY plane of the engineering coordinate system. Thus, with the increase of the antenna's pitch angle, the angle between the antenna's normal line projection on the XOY plane and the positive X-axis decreased first and then increased. It is reflected in Table 2 that the deviation value changes systematically from positive to negative, and the absolute value decreases to 0° first and then increases.

In addition, by comparison, we found that the change of temperature had no significant effect on the measurement of the antenna's attitude.

IV. DISCUSSION

A. DERIVATION OF THEORETICAL MAXIMUM DEVIATIONS OF OBSERVATIONS BETWEEN DIFFERENT INSTRUMENTS

In order to arrive at the theoretical maximum, it is necessary to make the possible deviations coplanar and collinear. In this way, it turns a three-dimensional problem into a planar one.

(1) Theoretical maximum deviation of observations between photogrammetry system and laser tracker

The theoretical model of the target ball's measurement by photogrammetry system and laser tracker, and the deviation generation is shown in Fig. 4. According to the figure, the theoretical maximum deviation of one target ball's observations between the two instruments is as formula (1):

$$D_{point} = U_{photo} + D_{p-centre} + U_{laser} + D_{l-centre} \quad (1)$$

Thus, the theoretical maximum deviation of the same length observation between the two instruments is as formula (2):

$$D_{lentgh} = D_{point} + D'_{point} \quad (2)$$

where U_{photo} is the single point measurement uncertainty of the photogrammetry system, $D_{p-centre}$ is the nominal optical centre deviation of photogrammetry's target ball, U_{laser} is the single point measurement uncertainty of laser tracker, $D_{l-centre}$ is the nominal optical centre deviation of laser tracker's target ball.

In this work, the photogrammetry system's observation distance was about 10 meters at most, while that of the laser tracker was about 5 meters. According to their nominal accuracy, their single point measurement uncertainty was about 0.05 mm. Furthermore, the nominal optical centre deviation of the photogrammetry's target ball and laser tracker's target ball was 0.01 mm. Therefore, it was calculated that the theoretical maximum deviation of target ball's coordinate measured by the two instruments is 0.12 mm, and the theoretical maximum deviation of the same length measured by the two instruments is 0.24 mm.

(2) Theoretical maximum deviation of observations between laser tracker and total station

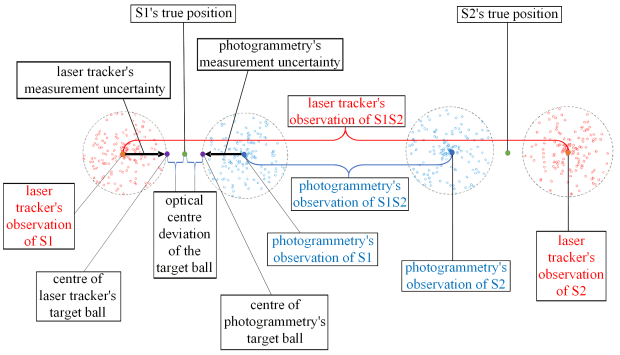

FIGURE 4. The theoretical model of the target ball's measurement by photogrammetry system and laser tracker, and the deviation generation.

The theoretical model of the reflector's measurement by laser tracker and total station, and the deviation generation is shown in Fig. 5. According to the figure, the theoretical maximum deviation of the reflector's observations between the two instruments is as formula (3):

$$D_{point} = U_{tstation} + U_{probe} + W_{cross} * \sqrt{2} \quad (3)$$

where $U_{tstation}$ is the single point measurement uncertainty of total station, U_{probe} is the single point measurement uncertainty of the handheld T-probe, W_{cross} is the width of cross marker on reflectors.

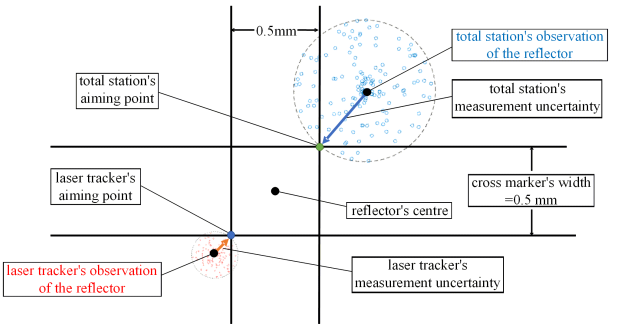

FIGURE 5. The theoretical model of the reflector's measurement by laser tracker and total station, and the deviation generation.

In this work, the nominal accuracy of the single point measurement by Leica's handheld T-probe is better than 0.06 mm within 30 meters. The cross marker's width on reflectors was about 0.5 mm. We estimated the single point measurement uncertainty of total station according to formula (4):

$$U_{tstation} = \sqrt{m_s^2 + (\frac{S_{AP} \cdot m_\beta}{\rho})^2} \quad (4)$$

where m_s and m_β are the nominal range accuracy and angular accuracy of total station, respectively. S_{AP} is the observation distance, $\rho = 206264$. As the total station's maximum observation distance was about 10 meters, it could be estimated that the single point measurement uncertainty of total station was about 0.85 mm.

Thus, according to formula (3), the theoretical maximum deviation of the reflector's observations between laser tracker and total station was approximately 1.62 mm.

B. ACCURACY EVALUATION OF PHOTOGRAMMETRIC OBSERVATIONS

The accuracy of photogrammetric observations was evaluated from the following two aspects.

(1) Root Mean Square Residual (RMSR) of the reference length and mark points' coordinates

The V-stars software obtained the RMSR of reference length and mark points' coordinates, as shown in Table 3.

As in Table 3, the maximum RMSR of reference length was 54 μm while that of mark points' coordinates was 59 μm.

TABLE 3. Root mean square residual of the reference length and mark points' coordinates in the photogrammetric callulation.

Temperature	Pitch angle	RMSR of the reference length (μm)	RMSR of the mark points' coordinates (μm)
5°C	0°	16	19
	15°	34	25
	30°	37	28
	45°	47	29
	60°	27	42
	75°	33	59
8°C	0°	19	27
	15°	12	27
	30°	19	27
	45°	26	31
	60°	14	40
	75°	12	53
12°C	0°	54	20
	15°	26	21
	30°	35	23
	45°	26	25
	60°	37	46
	75°	33	58
25°C	0°	21	23
	15°	26	27
	30°	17	25
	45°	45	29
	60°	20	54
	75°	49	58

In this work, the photogrammetry system's observation distance was about 10 meters at most. According to its nominal accuracy, the single point's measurement uncertainty was about 0.05 mm, and it was in accordance with the RMSR results of mark points' coordinates.

It was also found that the accuracy of the photogrammetric observation decreases with the increase of the antenna's pitch angle. It was speculated that the camera lens on the extension bar was vertically downward due to gravity. When the antenna is tilted, the camera lens could not face towards the antenna plane so that all the images taken were tilted. With the increase of the pitch angle, the images' tilt angle became larger, and so did the deformation of the circular marks in the images. Thus, the measurement accuracy was reduced. By comparing observations at different temperatures under the same pitch angle, we found that the temperature had no significant effect on the accuracy of photogrammetric measurement.

(2) Mutual deviations of the length observations between photogrammetry system and laser tracker

In each of the 24 observation groups, the photogrammetry system and laser tracker observed 5 target balls S1-S5, which were combined in pairs to form 10 length observations as S1S2, S1S3, ... S4S5. The mutual deviations between the same length observations by the two instruments were calculated, and the results are shown in Fig. 6.

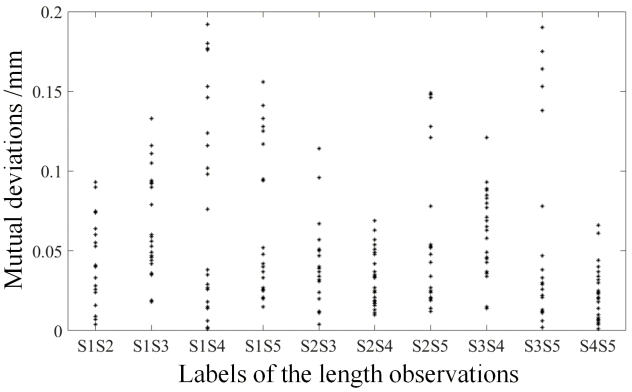

FIGURE 6. Mutual deviations of the length observations between photogrammetry system and laser tracker.

Through statistics, the maximum, minimum, and average of the mutual deviations were 0.192 mm, 0.001 mm, and 0.052 mm, respectively. As discussed in part A, the theoretical maximum deviation of the same length measured by the two instruments was 0.24 mm. Thus, the actual maximum mutual deviation of 0.192 mm was within reasonable limits.

In general, based on the two discussion parts, it was concluded that the photogrammetric method in this manuscript is accurate in the field measurement.

C. DEVIATIONS OF COORDINATE TRANSFORMATION

1) DEVIATIONS OF COORDINATE TRANSFORMATION FROM PHOTOGRAMMETRY SYSTEM TO LASER TRACKER

The maximum deviations between the converted and measured coordinates of target balls S1-S5 in the laser tracker's coordinate system in each observation group were calculated according to formula (5):

$$D_{max} = max[(X_{S_i} - x_{S_i})^2 + (Y_{S_i} - y_{S_i})^2 + (Z_{S_i} - z_{S_i})^2] \quad (5)$$

where $(X_{S_i}, Y_{S_i}, Z_{S_i})$ are the coordinates of points S_i measured by laser tracker, $(x_{S_i}, y_{S_i}, z_{S_i})$ are the converted coordinates from photogrammetry system to laser tracker, $i = 1, 2, \ldots, 5$.

Results are shown in Table 4. As discussed in part A, the theoretical maximum deviation of the target ball's coordinate measured by the two instruments is 0.12 mm under the ideal laboratory environment. It can be seen from Table 4 that the maximum deviation of a single point was 0.139 mm, which is 0.019 mm larger than the theoretical value.

Considering the effect of a complex environment on measurement accuracy, the theoretical maximum deviation of the target ball's coordinate measured by the two instruments

should be greater than 0.12 mm. Furthermore, considering that the antenna's flatness parameter RMS reached a millimeter or submillimeter level, which was far greater than the deviation, it was believed that the deviation would not significantly affect the fitting results of the antenna plane and the calculation of the antenna's pitch angles.

2) DEVIATIONS OF COORDINATE TRANSFORMATION FROM LASER TRACKER TO TOTAL STATION

The maximum deviations between the converted and measured coordinates of reflectors K1-K5 in the total station's coordinate system under different temperature conditions were calculated according to formula (6):

$$D_{max} = max[(X_{K_i} - x_{K_i})^2 + (Y_{K_i} - y_{K_i})^2 + (Z_{K_i} - z_{K_i})^2] \tag{6}$$

where $(X_{K_i}, Y_{K_i}, Z_{K_i})$ are the coordinates of points K_i measured by total station, $(x_{K_i}, y_{K_i}, z_{K_i})$ are the converted coordinates from laser tracker to total station, $i = 1, 2, \ldots, 5$.

Results are shown in Table 4. The maximum deviation between the converted and measured coordinates of reflectors is 1.037 mm, which is less than the two instruments' theoretical maximum deviation of observations. Therefore, in general, it is feasible that we measured the mark points on the antenna surface by photogrammetry system, and then converted the coordinates to laser tracker and total station's coordinate systems, instead of directly measuring the antenna plane by laser tracker or total station.

TABLE 4. The maximum deviations between the converted and measured coordinates of common points in laser tracker and total station's coordinate systems.

Temperature	Pitch angle	The maximum deviation between the converted and measured coordinates of target balls in laser tracker's coordinate system (mm)	The maximum deviation between the converted and measured coordinates of reflectors in total station's coordinate system (mm)
5°C	0°	0.067	1.004
	15°	0.056	
	30°	0.057	
	45°	0.062	
	60°	0.095	
	75°	0.105	
8°C	0°	0.111	1.012
	15°	0.131	
	30°	0.139	
	45°	0.119	
	60°	0.100	
	75°	0.129	
12°C	0°	0.067	1.037
	15°	0.065	
	30°	0.050	
	45°	0.053	
	60°	0.051	
	75°	0.051	
25°C	0°	0.117	0.944
	15°	0.138	
	30°	0.130	
	45°	0.111	
	60°	0.120	
	75°	0.125	

D. MEASUREMENT EFFICIENCY

The efficiency of this method was measured by the time it took to get the measurement work done. By statistic, under the condition of a certain temperature and pitch angle, it took one person about 2 hours to independently complete all the measurement, including observations by photogrammetry system, laser tracker, and total station, and all of the calculations. In contrast, if one took the measurement by traditional methods, such as total station, assuming that a single point targeting and measuring cost 2 minutes, then the measurement of all the 795 points on the antenna would cost 26.5 hours. Therefore, the efficiency of this method was greatly improved by about 10 times compared with traditional methods.

V. CONCLUSION

In this manuscript, a method for rapid measurement of the deformation and spatial attitude of a large, phased array radar antenna in a narrow space inside the radome by adopting the combination of industrial photogrammetry system, laser tracker and total station was proposed. The photogrammetric method detected the antenna's gravitational deformation sensitively, the maximum Root Mean Square Residual (RMSR) of the reference length was 54 μm, and that of the mark points was 59 μm, which was stably in line with its nominal accuracy. Deviations caused by coordinate transformation had no significant effect on the calculation of antenna's spatial attitude, for the maximum deviation between the converted and measured coordinates in laser tracker's coordinate system was 0.139 mm, and that in total station's coordinate system was 1.037 mm, both of which were within reasonable limits of the derived theoretical maximum deviations between different instruments. The maximum deviation between the calculated value and servo system's nominal value of antenna's pitch angle was 59.4″, and that of antenna's deflection angle was 91.87″. Through statistics and estimates, the efficiency of this method was greatly improved by about 10 times compared with traditional methods.

This method's uniqueness and superior characteristics are that the industrial surveying method is effectively combined with the traditional geodetic surveying method, which allows the deformation measurement data to be directly applied to the calculation of spatial position and attitude. It not only solves the problem that the industrial surveying method could not directly obtain the geographic position, but also gives full play to the advantages of the industrial surveying method, which is fast, high precision and with less blind area compared with the traditional geodetic surveying method. In fact, we believe that this technique is not limited to antennas or phased arrays but can also be applied to all other similar critical mechanical structures.

Further study should consider how to verify the accuracy of the mark points' coordinates after each coordinate transformation. Additionally, it is necessary to investigate the stability

and efficiency of this method applying to antennas with larger size.

ACKNOWLEDGMENT

The authors would like to acknowledge NRIET for providing the radar antenna mentioned in this manuscript for measurement and calculation, and for their help in the measurement process.

REFERENCES

[1] P. F. McManamon, T. A. Dorschner, D. L. Corkum, L. J. Friedman, D. S. Hobbs, M. Holz, S. Liberman, H. Q. Nguyen, D. P. Resler, R. C. Sharp, and E. A. Watson, "Optical phased array technology," *Proc. IEEE*, vol. 84, no. 2, pp. 268–298, Feb. 1996.

[2] R. J. Mailloux, "Phased array theory and technology," *Proc. IEEE*, vol. 70, no. 3, pp. 246–291, Mar. 1982.

[3] D. Dolfi, F. Michel-Gabriel, S. Bann, and J. P. Huignard, "Two-dimensional optical architecture for time-delay beam forming in a phased-array antenna," *Opt. Lett.*, vol. 16, no. 4, pp. 255–257, 1991.

[4] L. Stark, "Microwave theory of phased-array antennas—A review," *Proc. IEEE*, vol. 62, no. 12, pp. 1661–1701, Dec. 1974.

[5] E. Gorgucci, R. Bechini, L. Baldini, R. Cremonini, and V. Chandrasekar, "The influence of antenna radome on weather radar calibration and its real-time assessment," *J. Atmos. Ocean. Technol.*, vol. 30, no. 4, pp. 676–689, Apr. 2013.

[6] M. Frech, B. Lange, T. Mammen, J. Seltmann, C. Morehead, and J. Rowan, "Influence of a radome on antenna performance," *J. Atmos. Ocean. Technol.*, vol. 30, no. 2, pp. 313–324, Feb. 2013.

[7] A. Mancini, J. L. Salazar, R. M. Lebrón, and B. L. Cheong, "A novel instrument for real-time measurement of attenuation of weather radar radome including its outer Surface. Part I: The concept," *J. Atmos. Ocean. Technol.*, vol. 35, no. 5, pp. 953–973, May 2018.

[8] M. Kurri and A. Huuskonen, "Measurements of the transmission loss of a radome at different rain intensities," *J. Atmos. Ocean. Technol.*, vol. 25, no. 9, pp. 1590–1599, Sep. 2008.

[9] J. L. Salazar-Cerreño, V. Chandrasekar, J. M. Trabal, P. Siquera, R. Medina, E. Knapp, and D. J. McLaughlin, "A drop size distribution (DSD)-based model for evaluating the performance of wet radomes for dual-polarized radars," *J. Atmos. Ocean. Technol.*, vol. 31, no. 11, pp. 2409–2430, Nov. 2014.

[10] A. Mancini, J. L. Salazar, R. M. Lebrón, and B. L. Cheong, "A novel instrument for real-time measurement of attenuation of weather radar radome including its outer Surface. Part II: Applications," *J. Atmos. Ocean. Technol.*, vol. 35, no. 5, pp. 975–991, May 2018.

[11] D. S. Zrnic and R. J. Doviak, "System requirements for phased Array weather radar," in *Proc. NOAA/NSSL Rep*, 2005, pp. 1–24.

[12] N. Ukita, H. Ezawa, B. Ikenoue, and M. Saito, "Thermal and wind effects on the azimuth axis tilt of the ASTE 10-m antenna," *Publ. Natl. Astron. Obs. Jpn.*, vol. 10, pp. 25–33, Oct. 2007.

[13] A. Greve, D. Morris, J. Penalver, C. Thum, and M. Bremer, "The beam pattern of reflector antennas with buckled panels," *IEEE Trans. Antennas Propag.*, vol. 58, no. 3, pp. 959–962, Mar. 2010.

[14] J. Zhang, J. Huang, J. Zhou, C. Wang, and Y. Zhu, "A compensator for large antennas based on pointing error estimation under a wind load," *IEEE Trans. Control Syst. Technol.*, vol. 25, no. 5, pp. 1912–1920, Sep. 2017.

[15] B. Y. Duan and C. S. Wang, "Reflector antenna distortion analysis using MEFCM," *IEEE Trans. Antennas Propag.*, vol. 57, no. 10, pp. 3409–3413, Oct. 2009.

[16] P. Rocca, N. Anselmi, and A. Massa, "Interval arithmetic for pattern tolerance analysis of parabolic reflectors," *IEEE Trans. Antennas Propag.*, vol. 62, no. 10, pp. 4952–4960, Oct. 2014.

[17] P. Lian, B. Duan, W. Wang, B. Xiang, and N. Hu, "Effects of nonuniform surface errors along the radius on Reflector's radiation characteristic and its quality evaluation," *IEEE Trans. Antennas Propag.*, vol. 63, no. 5, pp. 2312–2316, May 2015.

[18] R. Kawabe, K. Kohno, Y. Tamura, T. Takekoshi, T. Oshima, and S. Ishii, "New 50-m-class single-dish telescope: Large submillimeter telescope (LST)," *Proc. SPIE*, vol. 9906, Aug. 2016, Art. no. 990626.

[19] S. Feng, C. Wang, B. Duan, and Y. Ban, "Design of tipping structure for 110 m high-precision radio telescope," *Acta Astronautica*, vol. 141, pp. 50–56, Dec. 2017.

[20] P. Lian, B. Duan, W. Wang, C. Wang, S. Zhang, and B. Xiang, "A pattern approximation method for distorted reflector antennas using piecewise linear fitting of the exponential error term," *IEEE Trans. Antennas Propag.*, vol. 63, no. 10, pp. 4546–4551, Oct. 2015.

[21] J. Ruze, "Antenna tolerance theory—A review," *Proc. IEEE*, vol. 54, no. 4, pp. 633–640, Apr. 1966.

[22] Y. Rahmat-Samii, "Surface diagnosis of large reflector antennas using microwave holographic metrology: An iterative approach," *Radio Sci.*, vol. 19, no. 5, pp. 1205–1217, Sep. 1984.

[23] I. Morison, "50 years of the Lovell telescope," *Astron. Geophys., J. Roy. Astronomical Soc.*, vol. 48, no. 5, pp. 5–23, 2007

[24] A. Greve, "Reflector surface measurements of the IRAM 30-m radio telescope," *Int. J. Infr. Millim. Waves*, vol. 7, no. 1, pp. 121–135, Jan. 1986.

[25] M. Morimoto, "Results from nobeyama radio observatory (NRO)—A progress report," *Astrophys. Space Sci.*, vol. 118, pp. 63–65, Jan. 1986.

[26] R. Hall, M. A. Goldman, D. H. Parker, and J. M. Payne, "Measurement program for the green bank telescope," *Int. Soc. Opt. Photon.*, vol. 3357, pp. 265–276, 1998.

[27] P. F. Goldsmith, "The second arecibo upgrade," *IEEE Potentials*, vol. 15, no. 3, pp. 38–43, Aug. 1996.

[28] R. W. Zhou, L. C. Zhu, J. W. Hu, and W. M. Li, "Study of a measurement algorithm for the surface of a single panel of the reflector of the FAST," *Astronomical Res. Technol.*, vol. 9, no. 1, pp. 14–20, 2012.

[29] F. Wenhao, "Control work in close range photogrammetry," *Geo-Spatial Inf. Sci.*, vol. 4, no. 4, pp. 66–72, Jan. 2001.

[30] C. Wei and X. F. Yu, "Estimation method of uncertainty of flatness error and determination of quantity of sampling points," *Metrology Meas. Technol.*, vol. 28, no. 6, pp. 43–45, 2008.

XIAO GUAN received the B.S. degree in geodesy and geomatics engineering from Wuhan University, Wuhan, China, in 2010, and the M.S. degree from the Institute of Seismology, China Earthquake Administration, Wuhan, in 2013. He is currently pursuing the Ph.D. degree in precise engineering surveying with the School of Geodesy and Geomatics, Wuhan University.

His research interest includes precise engineering surveying.

YAMING XU received the B.S. and M.S. degrees in engineering surveying from the Wuhan Technical University of Surveying and Mapping, Wuhan, China, in 1987 and 1990, respectively, and the Ph.D. degree in geodesy and surveying engineering from Wuhan University, Wuhan, in 2002.

He is currently a Professor with the School of Geodesy and Geomatics, Wuhan University. His research interests include precise engineering surveying and digital close photogrammetry.

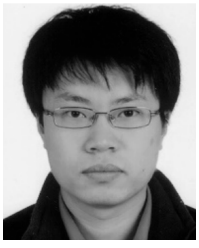

CHENG XING received the B.S. and Ph.D. degrees in geodesy and geomatics engineering from Wuhan University, Wuhan, China, in 2005 and 2011, respectively.

He is currently a Lecturer with the School of Geodesy and Geomatics, Wuhan University. His research interests include photogrammetry, precise image measurement, and ground-based synthetic aperture radar interferometric (GB-InSAR) deformation monitoring technology.